ORGANIC LETTERS

2011
Vol. 13, No. 22
6098–6101

Ratiometric Sensing of Fluoride Anions Based on a BODIPY-Coumarin Platform

Xiaowei Cao, Weiying Lin,* Quanxing Yu, and Jiaoliang Wang

State Key Laboratory of Chemo/Biosensing and Chemometrics, College of Chemistry and Chemical Engineering, Hunan University, Changsha, Hunan 410082, P. R. China

weiyinglin@hnu.edu.cn

Received September 26, 2011

ABSTRACT

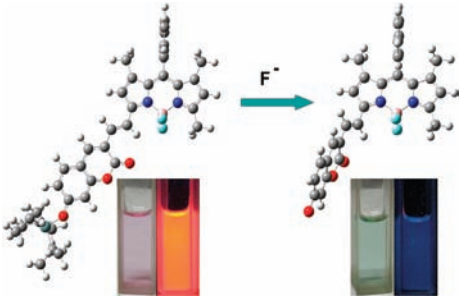

Based on a new coumarin-BODIPY platform, compound 4 was rationally designed and synthesized as a novel ratiometric fluorescent sensor for fluoride anions. The sensor exhibited a large red shift (88 nm) in absorption and a drastic ratiometric fluorescent response (I_{472}/I_{606} = 17.4) to fluoride anions. Density function theory and time-dependent density function theory calculations were conducted to rationalize the optical response of the sensor.

Construction of sensory molecules for recognition and sensing of anions is a forefront research topic in chemistry.[1] In particular, detection of anions by a fluorescent readout has attracted great attention in light of the advantages of fluorescence sensing including easy operation and high sensitivity.[2] Fluoride, the smallest anion with a high charge density, is an attractive target for sensor design due to its roles in dental care and other areas.[3]

Fluoride is a strong hydrogen bond acceptor and has a high affinity to silicon and boron. These unique physical and chemical properties have been widely exploited in the development of numerous fluorescent sensors for fluoride anions.[4] However, most of them are based on fluorescence measurement at a single wavelength, which may be influenced by variations in the sample environment. By contrast, ratiometric fluorescent sensors allow the measurement of emission intensities at two wavelengths, which should provide a built-in correction for environmental effects.[5] Thus, it is of interest to develop ratiometric fluorescent sensors for fluoride anions.

Difluoroboradiaza-*s*-indacene dyes (BODIPY) are highlighted with excellent photophysical and photochemical properties such as high fluorescence quantum yields, large extinction coefficients, and good photostability. In

(1) Schmidtchen, F. P.; Berger, M. *Chem. Rev.* **1997**, *97*, 1609–1646.
(2) (a) Martínez-Máñez, R.; Sancenón, F. *Chem. Rev.* **2003**, *103*, 4419–4476. (b) Li, A. –F.; Wang, J.-H.; Wang, F.; Jiang, Y.-B. *Chem. Soc. Rev.* **2010**, *39*, 3729–3745.
(3) (a) Kirk, K. L. *Biochemistry of the Halogens and Inorganic Halides*; Plenum Press: New York, 1991; p 58. (b) Kleerekoper, M. *Endocrinol. Metab. Clin. North Am.* **1998**, *27*, 441. (c) Dreisbuch, R. H. *Handbook of Poisoning*; Lange Medical Publishers: Los Altos, CA, 1980.
(4) For some examples, see: (a) Wade, C. R.; Broomsgrove, A. E. J.; Aldridge, S.; Gabbaï, F. P. *Chem. Rev.* **2010**, *110*, 3958–3984. (b) Cametti, M.; Rissanen, K. *Chem. Commun.* **2009**, 2809–2829. (c) Kumar, S.; Luxami, V.; Kumar, A. *Org. Lett.* **2008**, *10*, 5549–5552. (d) Qu, Y.; Hua, J.; Tian, H. *Org. Lett.* **2010**, *12*, 3320–3323. (e) Lu, Q.-S.; Dong, L.; Zhang, J.; Li, J.; Jiang, L.; Huang, Y.; Qin, S.; Hu, C.-W.; Yu, X.-Q. *Org. Lett.* **2009**, *11*, 669–672. (f) Bhalla, V.; Singh, H.; Kumar, M. *Org. Lett.* **2010**, *12*, 628–631. (g) Peng, X.; Wu, Y.; Fan, J.; Tian, M.; Han, K. *J. Org. Chem.* **2005**, *70*, 10524–10531. (h) Lin, Y.-C.; Chen, C.-T. *Org. Lett.* **2009**, *11*, 4858–4861. (i) Sokkalingam, P.; Lee, C.-H. *J. Org. Chem.* **2011**, *76*, 3820–3828. (j) Bozdemir, O. A.; Sozmen, F.; Buyukcakir, O.; Guliyev, R.; Cakmak, Y.; Akkaya, E. U. *Org. Lett.* **2010**, *12*, 1400–1403. (k) Kim, S. Y.; Hong, J.-I. *Org. Lett.* **2007**, *9*, 3109–3122. (l) Hu, R.; Feng, J.; Hu, D.; Wang, S.; Li, S.; Li, Y.; Yang, G. *Angew. Chem., Int. Ed.* **2010**, *49*, 4915–4918. (m) Zhang, J. F.; Lim, C. S.; Bhuniya, S.; Cho, B. R.; Kim, J. S. *Org. Lett.* **2011**, *13*, 1190–1193. (n) Xu, Z.; Kim, S. K.; Han, S. J.; Lee, C.; Kociok-Kohn, G.; James, T. D.; Yoon, J. *Eur. J. Org. Chem.* **2009**, *18*, 3058.
(5) Tsien, R. Y.; Harootunian, A. T. *Cell. Calcium.* **1990**, *11*, 93–100.
(6) (a) Loudet, A.; Burgess, K. *Chem. Rev.* **2007**, *107*, 4891–4932. (b) Jiao, L.; Yu, C.; Li, J.; Wang, Z.; Wu, M.; Hao, E. *J. Org. Chem.* **2009**, *74*, 7525–7528.

10.1021/ol202595t
Published on Web 10/27/2011

addition, the optical properties of BODIPY are tunable through chemical modifications on the dye core.[6] These favorable features render BODIPY as widely used as a fluorophore core for construction of fluorescent labels,[7] sensors,[8] light harvesting systems,[9] and photodynamic therapy agents.[10]

Coumarins are a classic type of push−pull dye, in which the intramolecular charge transfer (ICT) process from the electron donor to the acceptor proceeds upon excitation. Typically, for the efficient ICT, the donor and acceptor are located in the 7- and 3-position, respectively.[11] On the other hand, it is known that BODIPY dyes undergo an ICT process with a functional group at the 3′-position.[12]

ICT is an effective signaling mechanism employed in the design of ratiometric fluorescent sensors.[13] Thus, we envisioned that ratiometric fluorescent sensors for fluoride anions could be constructed by exploiting the ICT properties of both coumarin and BODIPY dyes. In this work, we present compound **4** based on a new BODIPY-coumarin platform as a novel candidate for ratiometric fluorescent fluoride sensing (Scheme 1). A triisopropylsilyl group was chosen as the potential reaction site for fluoride anions owing to the high affinity of fluoride to silicon.[14] The triisopropylsilyl group is judiciously placed in the 7-position of the coumarin unit. Upon reaction with fluoride anions, the triisopropylsilyl group may be unmasked, and compound **4** could be converted into the deprotected product (compound **3** in the phenolate form).[4i−m,15] As the phenolate group is a much stronger electron donor than the triisopropylsilyl group, the ICT efficiency should be markedly modulated upon interactions of compound **4** with fluoride anions. In addition, notably, the BODIPY-coumarin platform was carefully designed. With the triisopropylsilyl group positioned in the 7-position, the BODIPY was rationally placed in the 3-position of the coumarin unit for effective ICT. Thus, the coumarin unit is located in the 3′-position of the BODIPY dye, consistent with the typical design of ICT-based BODIPY sensors.[12]

Scheme 1. Design and Synthesis of Coumarin-BODIPY Conjugate **4** As a New Ratiometric Fluorescent Fluoride Sensor

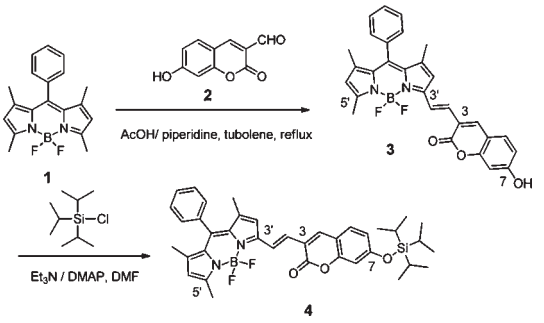

The coumarin-BODIPY-based compound **4** was readily synthesized in two steps (Scheme 1). The starting materials BODIPY **1** and coumarin aldehyde **2** were prepared based on the reported procedures.[6b,16] Condensation of BODIPY **1** with coumarin aldehyde **2** afforded the key intermediate **3**, which was further reacted with chlorotriisopropylsilane to give product **4**. All the new compounds were characterized by ^{1}H NMR, ^{13}C NMR, and HRMS.

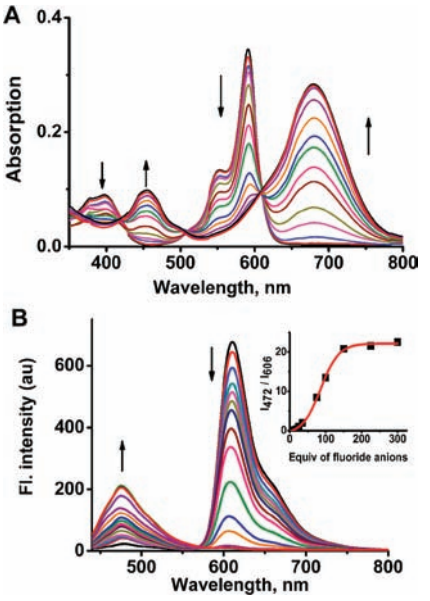

Figure 1. Absorption (A) and fluorescence (B) spectra of sensor **4** (3 μM) in DMSO in the presence of F^- anions (0−300 equiv). Excitation at 420 nm. The inset shows the fluorescence intensity ratio (I_{472} /I_{606}) as a function of equiv of fluoride anions.

With compound **4** in hand, we evaluated its response to F^- anions by absorption and emission spectroscopy. The free sensor **4** displayed two major absorption bands at 398 and 592 nm. However, addition of F^- induced a large red shift in both the absorption peaks (Figure 1A), consistent with the ICT signaling mechanism as designed.

(7) Haugland, R. P. *The Handbook-A Guide to Fluorescent Probes and Labeling Technologies*, 10th ed.; Invitrogen Corp.: 2005.

(8) (a) Boens, N.; Leen, V.; Dehaen, W. *Chem. Soc. Rev.*, DOI: 10.1039/c1cs15132k. (b) Kamiya, M.; Johnsson, K. *Anal. Chem.* **2010**, *82*, 6472–6479. (c) Rosenthal, J.; Lippard, S. J. *J. Am. Chem. Soc.* **2010**, *132*, 5536–5537. (d) Sun, Z.-N.; Wang, H.-L.; Liu, F.-Q.; Chen, Y.; Kwong, P.; Tam, H.; Yang, D. *Org. Lett.* **2009**, *11*, 1887–1890. (e) Ojida, A.; Sakamoto, T.; Inoue, M.; Fujishima, S.; Lippens, G.; Hamachi, I. *J. Am. Chem. Soc.* **2009**, *131*, 6543–6548. (f) Matsumoto, T.; Urano, Y.; Shoda, T.; Kojima, H.; Nagano, T. *Org. Lett.* **2007**, *9*, 3375–3377. (g) Kennedy, D. P.; Kormos, C. M.; Burdette, S. C. *J. Am. Chem. Soc.* **2009**, *131*, 8578–8586.

(9) (a) Ziessel, R.; Harriman, A. *Chem. Commun.* **2011**, *47*, 611–631. (b) Zhang, X.; Xiao, Y.; Qian, X. *Org. Lett.* **2008**, *10*, 29–32.

(10) Atilgan, S.; Ekmekci, Z.; Dogan, A. L.; Guc, D.; Akkaya, E. U. *Chem. Commun.* **2006**, 4398–4400.

(11) (a) Signore, G.; Nifosì, R.; Albertazzi, L.; Storti, B.; Bizzarri, R. *J. Am. Chem. Soc.* **2010**, *132*, 1276–1288. (b) Wang, J.; Qian, X.; Cui, J. *J. Org. Chem.* **2006**, *71*, 4308–4311.

(12) (a) Deniz, E.; Isbasar, G. C.; Bozdemir, Ö . A.; Yildirim, T. L.; Siemiarczuk, A.; Akkaya, E. U. *Org. Lett.* **2008**, *10*, 3401–3403. (b) Peng, X.; Du, J.; Fan, J.; Wang, J.; Wu, Y.; Zhao, J.; Sun, S.; Xu, T. *J. Am. Chem. Soc.* **2007**, *129*, 1500–1501.

(13) Lakowicz, J. R. *Topics in Fluorescence Spectroscopy, Vol. 4: Probe Design and Chemical Sensing*; Kluwer Academic Publishers: New York, 2002.

(14) *Protective Groups in Organic Synthesis*, 3rd ed.; Greene, T. W., Wuts, P. G. M., Eds.; Wiley: New York, 1999; pp 113−148.

Three well-defined isosbestic points at 420, 510, and 612 nm were observed, indicating the formation of a new species upon treatment of sensor **4** with F^-. In good agreement with the findings in absorption, the sensor exhibited a ratiometric fluorescent response to F^- anions. Upon excitation at 420 nm, the free sensor displayed an intense emission band at 606 nm. However, as shown in Figure 1B, addition of F^- elicited a drastic decrease in the emission at 606 nm and simultaneous appearance of a new emission band at 472 nm, attributed to the local emission (LE). Thus, the sensor provided a significant ratiometric fluorescent response (I_{472}/I_{606}) to F^- anions (inset in Figure 1B). However, upon excitation at 612 nm, treatment of the sensor with F^- anions afforded no discernible emission. This is the typical behavior of BODIPY-based ICT sensors: the ICT emission band is almost nonfluorescent when excited at the ICT absorption band.[4j] A mass spectrometry analysis (Figure S1) confirms that the F^- anion-triggered spectroscopic changes are indeed due to the removal of the triisopropylsilane and thus the formation of the deprotected product. The electron donating ability of the phenolate group is much stronger than that of the silane group, thereby a large red shift is observed in the absorption profiles upon treatment of the sensor with F^- anions. The detection limit ($S/N = 3$) for sensor **4** was calculated to be 0.12 μM, and it reacted with fluoride very rapidly (Figure S2). We also evaluated the effect of water on the fluorescence response of sensor **4** to fluoride anions. When the water content increases, the deprotected reaction becomes less active due to the strong hydrogen bonding between water and fluoride (Figure S3).

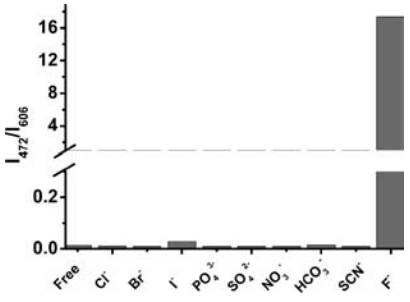

Figure 2. Emission ratios (I_{472}/I_{606}) of sensor **4** (3 μM) in the presence of various relevant analytes (150 equiv for fluoride anions, 300 equiv for other anions). Excitation at 420 nm.

Sensor **4** (3 μM) was treated with various anion species represented by Cl^-, Br^-, I^-, NO_3^-, SO_4^{2-}, HCO_3^-, PO_4^{3-}, and SCN^- to investigate the selectivity. The sensor displayed a large ratiometric signal ($I_{472}/I_{606} = 17.4$) to F^- anions (Figures 2 and S4). By contrast, other analytes only induced a minimum ratiometric response with $I_{472}/I_{606} < 0.03$. These results indicate that the sensor is highly selective to F^- over other species tested. To examine whether sensor **4** could still retain the sensing response to F^- under the potential competition of relevant analytes, the sensor (3 μM) was treated with F^- in the presence of Cl^-, Br^-, I^-, NO_3^-, SO_4^{2-}, HCO_3^-, PO_4^{3-}, CN^-, or SCN^-. As displayed in Figures 3 and S5, all the relevant analytes tested have virtually no influence on the fluorescent detection of F^-. Thus, sensor **4** seems to be useful for selectively sensing F^- even with these relevant analytes. Notably, the big red shift in the absorption and the large ratiometric fluorescent response render the sensor suitable for detection of F^- anions by simple visual inspection (Figure 4).

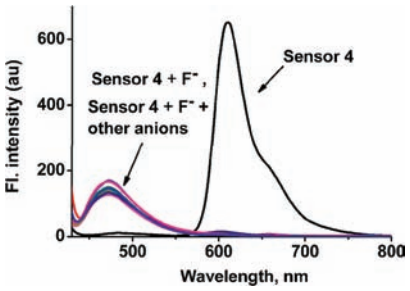

Figure 3. Fluorescent spectra of sensor **4** (3 μM) to F^- anions (150 equiv) in the presence of 300 equiv of various relevant analytes (Cl^-, Br^-, I^-, NO_3^-, SO_4^{2-}, HCO_3^-, PO_4^{3-}, CN^-, or SCN^-) in DMSO.

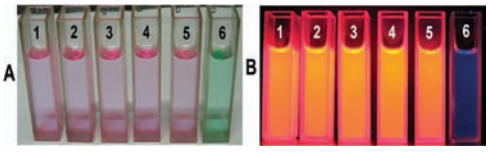

Figure 4. Visible color (A) and visual fluorescence color (B) changes of sensor **4** (3 μM) with various relevant analytes (150 equiv for F^-, 300 equiv for other anions) in DMSO: (1) Free sensor **4**; (2) sensor **4** + Cl^-; (3) sensor **4** + Br^-; (4) sensor **4** + I^-; (5) sensor **4** + SCN^-; (6) sensor **4** + F^-. The visual fluorescence color was obtained with excitation at 365 nm using a hand-held UV lamp.

To get insight into the optical response of sensor **4** to F^- anions, the sensor and the corresponding deprotected product were examined by density function theory (DFT) and time-dependent density function theory (TD-DFT) calculations at the B3LYP/6-31G(d) level of the Guassian 03 program. As shown in Figure 5, for sensor **4**, both the HOMO and LUMO are distributed at the coumarin-ethenyl bridge-BODIPY scaffold. Thus, the

(15) (a) Zhu, B.; Yuan, F.; Li, R.; Li, Y.; Wei, Q.; Ma, Z.; Du, B.; Zhang, X. *Chem. Commun.* **2011**, *47*, 7098–7100. (b) Ren, J.; Wu, Z.; Zhou, Y.; Li, Y.; Xu, Z. *Dye. Pigment.* **2011**, *91*, 442–445. (c) Yang, X.-F.; Ye, S.-J.; Bai, Q.; Wang, X.-Q. *J. Fluoresc.* **2007**, *17*, 81–87. (d) Kim, S. Y.; Park, J.; Koh, M.; Park, S. B.; Hong, J.-I. *Chem. Commun.* **2009**, 4735–4737.

(16) Lim, N. C.; Schuster, J. V.; Porto, M. C.; Tanudra, M. A.; Yao, L.; Freake, H. C.; Brückner, C. *Inorg. Chem.* **2005**, *44*, 2018–2030.

ICT character of the sensor is only modest. By sharp contrast, for the deprotected product, the HOMO is mainly located between the coumarin moiety and the ethenyl bridge, and the LUMO is mostly located between the BODIPY unit and the ethenyl bridge. This indicates that the deprotected product bears strong ICT character from the coumarin moiety to the BODIPY unit, consistent with the design strategy. Furthermore, the energy gap between the HOMO and LUMO of the deprotected product is much smaller than that of sensor **4**, in good agreement with the red shift in the absorption observed upon treatment of sensor **4** with F^- anions.

To shed light on the formation of the local emission (LE) band at 472 nm with excitation at 420 nm upon incubation of the sensor with F^- anions, sensor **4** and the deprotected product were optimized by DFT calculations with the B3LYP exchange functional employing 6-31G(d) basis sets using a suite of Gaussian 03 programs. As displayed in Figure S6, the optimized structure of the deprotected product has a dihedral angle of about −77.2° between the coumarin and the BODIPY moieties, whereas the sensor is essentially planar between the coumarin and the BODIPY moieties with a dihedral angle of −5.9°. Thus, the formation of the LE emission band at 472 nm in the deprotected product is likely due to the nonplanar and deconjugated character. In addition, we also performed time-dependent density function theory (TD-DFT) calculations for both the deprotected product and the sensor. In the case of the deprotected product, TD-DFT calculations provide a calculated absorption band at 414 nm belonging to the $S_0 \rightarrow S_{11}$ energy state (Table S1). This is consistent with the absorbance band at 456 nm obtained experimentally. The transitions of HOMO−3→LUMO, HOMO−2→LUMO, HOMO→LUMO+4, and HOMO→LUMO+9 contribute 27.4%, 12.0%, 46.4%, and 15.4% of the $S_0 \rightarrow S_{11}$ energy state, respectively. The main contribution transition for the $S_0 \rightarrow S_{11}$ energy state comes from HOMO→LUMO+4. Notably, both the HOMO and LUMO+4 orbitals are mainly located at the coumarin moiety (Figure S7), which translates the LE emission from the coumarin moiety in the deprotected product. Notably, the emission profile of the LE band highly resembles that of the control coumarin **2** (Figure S8), further confirming that the LE band originates from the coumarin moiety in the deprotected product. By contrast, as shown in Figure S9, no allowed singlet state transitions are located on the coumarin moiety in sensor **4**. Thus, the LE emission from the coumarin moiety is not present in the sensor.

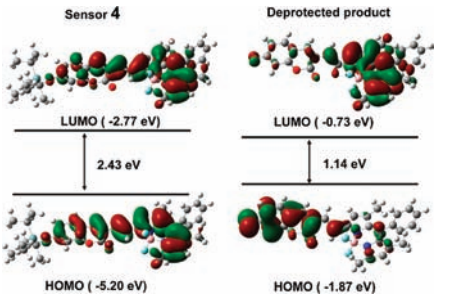

Figure 5. HOMO−LUMO energy levels and the interfacial plots of the orbitals for sensor **4** and the deprotected product.

In summary, we have rationally designed and synthesized compound **4** based on the new coumarin-BODIPY platform as a novel ratiometric fluorescent sensor for fluoride anions. The sensor exhibited a large red shift (88 nm) in absorption and a drastic ratiometric fluorescent response (I_{472}/I_{606} = 17.4) to fluoride anions. In addition, the sensor is highly selective for fluoride anions. The large red shift in the absorption and the ratiometric fluorescent response render the sensor suitable for detection of F^- anions by simple visual inspection. Density function theory and time-dependent density function theory calculations were conducted to rationalize the optical response of the sensor. We expect that the unique ICT character of the coumarin-BODIPY platform will be widely employed to construct a wide variety of ratiometric fluorescent sensors based on the ICT signaling mechanism.

Acknowledgment. This work was financially supported by NSFC (20872032, 20972044, 21172063), NCET (08-0175), the Doctoral Fund of Chinese Ministry of Education (20100161110008), and the Fundamental Research Funds for the Central Universities, Hunan University.

Supporting Information Available. Experimental procedures, some spectra of the sensor, and the quantum calculation data. This material is available free of charge via the Internet at http://pubs.acs.org.